JACS
JOURNAL OF THE AMERICAN CHEMICAL SOCIETY

Perspective

pubs.acs.org/JACS

Relationships between Lead Halide Perovskite Thin-Film Fabrication, Morphology, and Performance in Solar Cells

Alexander Sharenko* and Michael F. Toney*

†Stanford Synchrotron Radiation Lightsource, SLAC National Accelerator Laboratory, Menlo Park, California 94025, United States

ABSTRACT: Solution-processed lead halide perovskite thin-film solar cells have achieved power conversion efficiencies comparable to those obtained with several commercial photovoltaic technologies in a remarkably short period of time. This rapid rise in device efficiency is largely the result of the development of fabrication protocols capable of producing continuous, smooth perovskite films with micrometer-sized grains. Further developments in film fabrication and morphological control are necessary, however, in order for perovskite solar cells to reliably and reproducibly approach their thermodynamic efficiency limit. This Perspective discusses the fabrication of lead halide perovskite thin films, while highlighting the processing−property−performance relationships that have emerged from the literature, and from this knowledge, suggests future research directions.

1. INTRODUCTION

Lead halide perovskites are a relatively new class of photoactive material. Photovoltaic devices utilizing lead halide perovskites as the light absorbing layer have experienced a dramatic increase in power conversion efficiency (PCE) since their emergence over the past ∼5 years.[1] Currently, lead halide perovskite photovoltaic devices exhibit PCEs as high as ∼20%,[2] comparable to more established thin-film inorganic photovoltaic materials such as copper indium gallium selenide and cadmium telluride.[3] This high photovoltaic efficiency is in large part enabled by the intrinsically favorable optoelectronic properties of lead halide perovskites. Lead halide perovskites exhibit high absorption coefficients and remarkably sharp absorption edges.[4] Additionally, theory suggests their point defects are electrically benign.[5,6] Setting lead halide perovskite materials apart from other high-efficiency photovoltaic materials, however, is their ability to be readily solution-processed from soluble inorganic and organic precursor materials or fabricated with low-temperature sublimation processes. Even with these favorable intrinsic material properties, high photovoltaic efficiencies were not achieved with solution-processed lead halide perovskite films until it was discovered how to fabricate high-quality solution-processed thin films. This Perspective will provide a short history of this discovery process as well as elucidate some of the processing−property−performance relationships established as part of this effort. A more complete historical overview of the field as well as a discussion of some of the challenges facing this field beyond film fabrication and morphology, such as photocurrent hysteresis[7,8] and environmental stability,[9,10] can be found elsewhere.[1,11]

Multiple different solution-based fabrication methodologies have been developed for lead halide perovskite materials. Synthesis of the lead halide perovskite and film formation happens simultaneously or is at least closely coupled in many of these fabrication protocols, complicating the development of processing−property−performance relationships for this class of material. Each fabrication protocol produces a different perovskite film morphology (grain size/shape, film roughness, surface coverage, etc.), and in turn these different morphologies influence the optoelectronic properties of the film, e.g., carrier diffusion lengths, charge carrier mobilities, defect states, etc. Thus, even given the difficulties associated with decoupling synthetic and film formation effects, processing−property−performance relationships have emerged from the ever growing body of literature on the fabrication of thin-film lead halide perovskite solar cells. It is then the goal of this Perspective to present pertinent examples from the literature and highlight some of the relationships between film fabrication protocol, film morphology, and the resultant optoelectronic properties of these films and devices in order to help move this field toward the goal of reliably and reproducibly producing lead halide perovskite photovoltaic devices that approach their Shockley−Queisser efficiency limit. Generally, examples will be confined to the fabrication of planar lead halide perovskite thin films given their recent rise in prominence over mesoporous device architectures. The most common lead halide perovskite, methylammonium lead iodide ($MAPbI_3$), will serve as the basis of the majority of the discussion, but systems utilizing other organic or halide ions will be mentioned where appropriate.

This Perspective is largely organized as a discussion of the major thin-film perovskite fabrication techniques, providing a mechanistic understanding of how each protocol produces its specific perovskite morphology. Additionally, the effect of humidity on fabrication is specifically discussed, and desirable morphological traits are identified. This Perspective is by no means comprehensive, but instead it aims to highlight some of the more recent, compelling areas of thin-film lead halide perovskite film fabrication, while providing additional insight on the highlighted works so as to guide future research efforts.

2. TWO-STEP FABRICATION PROTOCOLS

All lead halide perovskite fabrication protocols combine an organic salt with a lead salt to produce a lead halide perovskite thin film. Generally, these precursors either can be combined together in a common solution or can be combined from separate solutions. These general classes of fabrication

Received: October 13, 2015
Published: November 20, 2015

DOI: 10.1021/jacs.5b10723
J. Am. Chem. Soc. 2016, 138, 463−470

protocols are referred to as one- and two-step fabrication protocols, respectively. The simplest two-step fabrication protocol consists of depositing a film of a lead salt, commonly PbI_2, and then immersing this lead salt film into a solution containing an organic salt. The solvent must be carefully chosen so as not to dissolve the already deposited lead salt film or the developing perovskite film. Liang and co-workers at IBM Watson Research Center were the first to demonstrate this technique for the fabrication of lead halide perovskite thin films.[12] Fifteen years later Burschka et al. adapted this methodology to work with a mesoporous TiO_2 framework to construct the first high-efficiency (~15% PCE) solution-processed perovskite solar cell.[13] Liu and Kelly then further adapted this fabrication protocol to make the first high-efficiency solution-processed planar lead halide perovskite solar cells.[14]

The two-step dipping fabrication protocol produces a thin-film morphology consisting of what appear to be many discrete lead halide perovskite particles with dimension ranging from ~50 to ~500 nm. The size distribution of these perovskite particles can be significantly narrowed by starting with an amorphous PbI_2 film as opposed to a crystalline PbI_2 film (Figure 1).[15] Whether the PbI_2 film is amorphous or crystalline

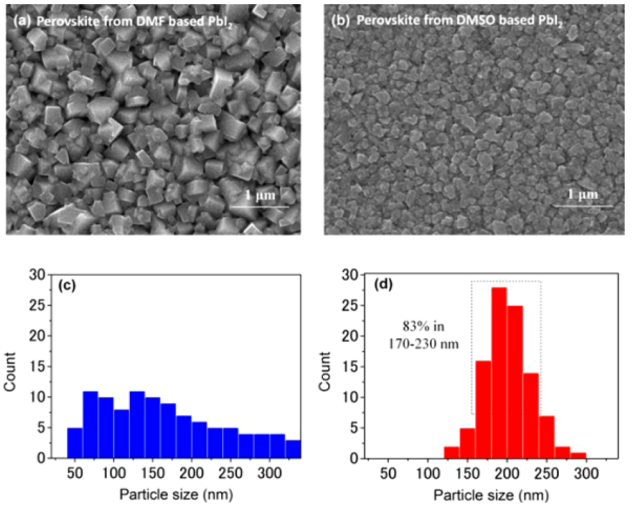

Figure 1. (a,b) Scanning electron microscopy images of $MAPbI_3$ synthesized using the two-step dipping method from a crystalline and amorphous PbI_2 film, respectively. (c,d) Grain size distribution of images in (a) and (b), respectively. Reproduced with permission from ref 15. Copyright 2014 The Royal Society of Chemistry.

can be controlled by the solvent used to cast the PbI_2 film. Casting the PbI_2 film from dimethylformamide (DMF) produces a crystalline film, but casting from dimethyl sulfoxide (DMSO) produces an amorphous film as DMSO molecules complex with PbI_2 in solution to prevent crystallization. These more narrowly distributed perovskite particles were reported to produce higher efficiency, more reproducible solar cells. This example demonstrates how the final lead halide perovskite morphology is strongly dependent on the morphology of the initial PbI_2 layer when using a two-step fabrication protocol. This is further demonstrated in work by Yang et al., where HI and HCl were added to the PbI_2 solution to change the morphology of the corresponding PbI_2 film.[16] The HI and HCl led to a more continuous, smaller grained PbI_2 film, which in turn led to a more continuous $MAPbI_3$ film when converted using the two-step dipping method. Clearly, controlling the PbI_2 morphology is a viable strategy for controlling the final perovskite morphology when using a two-step method.

Another two-step fabrication protocol is the bilayer interdiffusion method developed by the Huang group.[17,18] In this protocol, a layer of PbI_2 is deposited, and then a layer of MAI is deposited on top of the PbI_2 layer from isopropanol so as not to dissolve the underlying PbI_2 layer. This PbI_2/MAI bilayer is then annealed to drive diffusion of the two reactants and concomitant formation of $MAPbI_3$. This fabrication protocol produces a continuous, fully converted $MAPbI_3$ film after approximately 60 min of annealing at 100 °C. The grain size of films prepared in this manner can be increased by using a non-wetting substrate, which leads to slightly increased short-circuit current density and fill factor.[19] The grain size can also be increased by using an MAI/MACl blend solution instead of an MAI solution to perform a series of coating and annealing cycles on the initial PbI_2 film (Figure 2).[20] This procedure leads to abnormal grain growth and was shown to produce select grains as large as 3 μm, which led to a longer charge carrier recombination lifetime. The abnormal grain growth and the resultant large grains exhibited with the introduction of MACl into the coating solution could be the result of chloride-containing precipitates acting as nucleation sites, similar to what has been suggested to occur in one-step fabrication protocols (discussed further below).[21] As with the two-step dipping fabrication, controlling the PbI_2 layer morphology is an effective strategy to control the morphology of perovskite films produced by the interdiffusion bilayer technique. To this end, Wu et al. introduced controlled amounts of H_2O into PbI_2/DMF solutions, which in turn led to more fully dissolved solutions that produced highly crystalline, more homogeneous, smoother PbI_2 films.[22] These crystalline, homogeneous, smooth PbI_2 films produced highly uniform, smooth $MAPbI_3$ films with increased PCE compared to when H_2O was not used as a processing additive.

3. ONE-STEP FABRICATION PROTOCOLS

The one-step fabrication protocol consists of mixing both the inorganic and organic precursors in a single solution, casting a film from this solution, and then annealing this film to drive complete formation of the perovskite phase. Initially, solution-processed planar perovskite solar cells exhibited significantly lower PCE than thermally evaporated perovskite solar cells (7% vs 15%).[23] This disparity could be explained by the difficulties associated with producing a continuous, compact, smooth perovskite film using the one-step method. Discontinuous, rough films lead to electrical shorts, increased device dark current, and poor light absorption, which all lower device PCE. Decreasing the annealing temperature and processing in a nitrogen glove box environment led to increased film coverage and PCE, but PCEs of planar devices that utilized one-step fabrication were still lower than thermally evaporated devices.[24] One of the greatest challenges of one-step perovskite fabrication has therefore been the ability to easily form continuous, smooth films. Casting a 1:1 molar PbI_2:MAI solution from DMF results in a discontinuous, needle-like morphology.[25] Several work-arounds have been developed that allow a more continuous, smooth film to be cast using the one-step method. Casting from a solution containing a molar excess of MAI results in a smoother, more continuous film (Figure 3).[25,26] Additionally, several solvent additives have been discovered that also result in smoother, continuous films

DOI: 10.1021/jacs.5b10723
J. Am. Chem. Soc. 2016, 138, 463−470

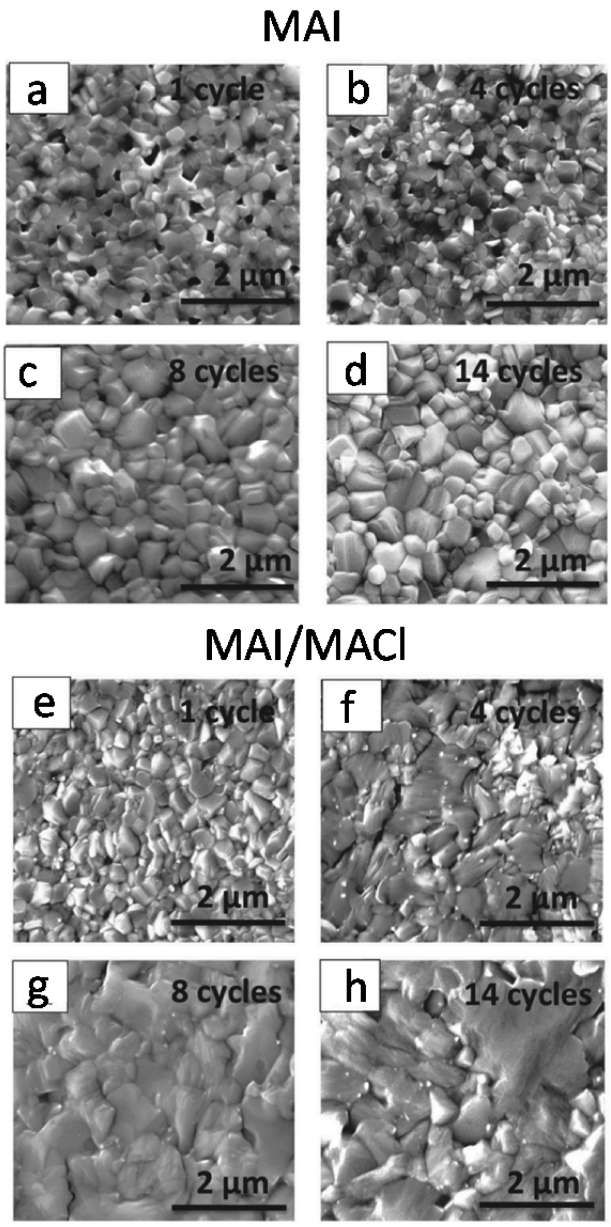

Figure 2. $MAPbI_3$ films synthesized by two-step method using either an MAI (a–d) or an MAI/MACl solution (e–h). Adapted from ref 20 with permission from The Royal Society of Chemistry.

when added in small amounts to PbI_2/MAI solutions. Several alkyl halides have been shown to lead to improved film coverage and thus PCE because of significantly higher fill factors.[27,28] HI and HCl have also shown dramatic improvements in film coverage when used as solution processing additives.[29−32] Yan et al. have further developed the theory of one-step perovskite processing by proposing PbI_2 and MAI form an extended colloidal network in DMF, as is common with sol−gel processing of some inorganic materials.[26] They used UV−vis spectroscopy and dynamic light scattering to observe how the solution absorption band edge and particle size changed as a function of inorganic/organic precursor blend ratio and concentration. They hypothesize that adding excess MAI and/or MACl leads to improved film coverage because the additional halogen ions help break up the PbI_2 colloidal network in solution via the formation of lead coordination complexes such as $[PbI_3]^-$ or $[PbI_2Cl]^-$.[33,34] This theory would also explain why the addition of HI, HCl and, to a lesser degree, alkyl halides leads to smoother, more continuous films as they would also serve as a source of additional halide ions to disrupt the colloidal network. The aggregates associated with the PbI_2 colloidal network may lead to non-uniform nucleation over the substrate, which is why efforts to improve the lead precursor's solubility, i.e., disrupting the extended colloidal PbI_2 network, seem to lead to more uniform nucleation and therefore smoother, more continuous films.

Much initial work with one-step fabrication protocol focused on using $PbCl_2$ as the lead source.[23,24] This was largely due to early observations that $MAPbI_3$ films made using $PbCl_2$ as opposed to PbI_2 exhibited significantly longer electron and hole diffusion lengths and so greater PCE in planar devices where charge carriers have to diffuse much farther than in mesoporous scaffolds before being collected by electrodes.[35] The specific role that chlorine plays in the fabrication process and why it leads to perovskite films with superior optoelectronic properties have been much debated since this initial observation. Density functional theory simulations have been used to suggest that chloride ions in $PbCl_2$-derived perovskite films may act as electronic dopants, thus improving charge transport.[36] Alternatively, the presence of chloride ions has been suggested to control film morphology during processing either by facilitating the release of MA ions at a reduced temperature during annealing[37] or by acting as a nucleating agent during thermal annealing,[21] thus leading to a denser layer of smaller perovskite crystallites or enhanced film crystallinity. Williams et al. demonstrated that how chloride ions are introduced during the fabrication process (MACl vs $PbCl_2$) influences final film morphology, possibly because of how these different precursors affect complex ion equilibria in precursor solutions.[34] Unger and co-workers used X-ray fluorescence measurements to show that the chlorine concentration in $PbCl_2$-derived perovskite films decreases with increasing annealing time.[38] Attempts to quantify chloride ion concentration in fully formed $PbCl_2$-derived perovskite films have shown amounts ranging from less than 300 ppm to as much as a mole fraction of 0.22 relative to iodine.[37,39−42] The most recent work in the field, however, demonstrates that the presence of chloride ions during

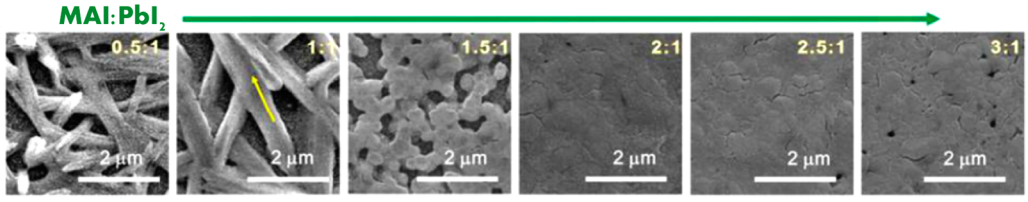

Figure 3. $MAPbI_3$ films prepared with a one-step fabrication protocol with different molar ratios of MAI and PbI_2 in solution. Reprinted with permission from ref 26. Copyright 2015 American Chemical Society.

DOI: 10.1021/jacs.5b10723
J. Am. Chem. Soc. 2016, 138, 463−470

processing or in the final perovskite film is not essential for the fabrication of high-performance perovskite solar cells.[2]

Specifically, Zhang and co-workers demonstrated that perovskite solar cells can be fabricated using a one-step protocol utilizing $Pb(CH_3COO)_2$ as the lead source with very similar performance compared to $PbCl_2$-derived devices.[39] This is possibly because in both cases the byproduct of the perovskite reaction ($MACH_3COO$ and MACl when using $Pb(CH_3COO)_2$ and $PbCl_2$, respectively) thermally decomposes at relatively low annealing temperatures, thus accelerating crystallization kinetics and allowing perovskite formation before excessive coarsening and roughening occur.[43] Additionally, some of the current highest performing perovskite solar cells utilize PbI_2 as the lead source and rely on solvent engineering methods (discussed more below) or solvent additives to achieve desirable morphologies. These recent results suggest that, while chloride ions may have some unique, beneficial optoelectronic functionality in lead halide perovskite films, smooth and continuous films with micrometer-sized grains fabricated without the use of any chloride ion source demonstrate similarly desirable optoelectronic properties.

4. SOLVENT ENGINEERING

Solvent engineering is perhaps the most recent development in thin-film perovskite fabrication. It can be thought of as combining the advantages of both the one- and two-step fabrication protocols. In two-step fabrication, film formation and perovskite synthesis are largely decoupled by first forming a film of the inorganic precursor and then converting this film to the perovskite, ensuring good film coverage. In contrast, one-step fabrication forms a film and synthesizes the lead halide perovskite in a single step, making it a quicker, more straightforward process. By combining both organic and inorganic precursors in solution, however, control is lost over how the chemical synthesis of the perovskite proceeds, likely contributing to the incomplete film coverage commonly exhibited by this fabrication protocol. Solvent engineering is a class of fabrication techniques that combine both precursors in solution, but that also purposely introduces a solvent that coordinates with PbI_2 in order to form PbI_2–solvent complexes and thus prevent further chemistry from happening in solution. A film of this precursor–solvent complex is then cast and subsequently converted to the lead halide perovskite. This technique was first introduced by Jeon et al., wherein toluene was dripped on the film during spin-coating in order to stabilize the formation of a crystalline, transparent MAI–PbI_2–DMSO complex that was then converted to a smooth, continuous perovskite film via thermal annealing.[44] Ahn and co-workers modified the solvent engineering method by washing with diethyl ether during spin-coating instead of toluene, producing very smooth, compact $MAPbI_3$ films that made solar cells with an average PCE of 18.3%.[45] In that work, the PbI_2–DMSO complex may just prevent the formation of colloidal PbI_2 and therefore lead to more uniform nucleation, much like the mechanism suggested for solvent additives. Alternatively, as suggested by the authors, the diethyl ether wash in conjunction with the formation of a PbI_2–DMSO complex may prevent differing crystallization rates between lower-solubility PbI_2 and higher solubility MAI, which may otherwise contribute to the poor surface coverage and needle-like morphology associated with 1:1 molar PbI_2:MAI solutions cast from DMF. This latter explanation is consistent with other work where smooth, continuous lead halide perovskite films are synthesized from 1:1 PbI_2:MAI DMF solutions by accelerating film drying via a stream of nitrogen gas,[46] casting on a heated substrate,[47] or immediately washing the drying film with an anti-solvent.[48] The acceleration in film drying that these treatments cause would likely also prevent the crystallization of PbI_2 and MAI on significantly different time scales and therefore encourage more uniform nucleation across the substrate. Yang and co-workers modified aspects of the solvent engineering process developed by Jeon et al. to produce a perovskite solar cell utilizing an alternative organic cation with a maximum PCE of 20.1%.[2] They refer to their fabrication process as an intramolecular exchange process (IEP) as the organic cation displaces DMSO molecules in a PbI_2–DMSO complex to form the lead halide perovskite. This process produced a film with much larger grains compared to the two-step interdiffusion method, leading to higher short-circuit current density and fill factor (Figure 4). It is not well understood how this IEP alters the

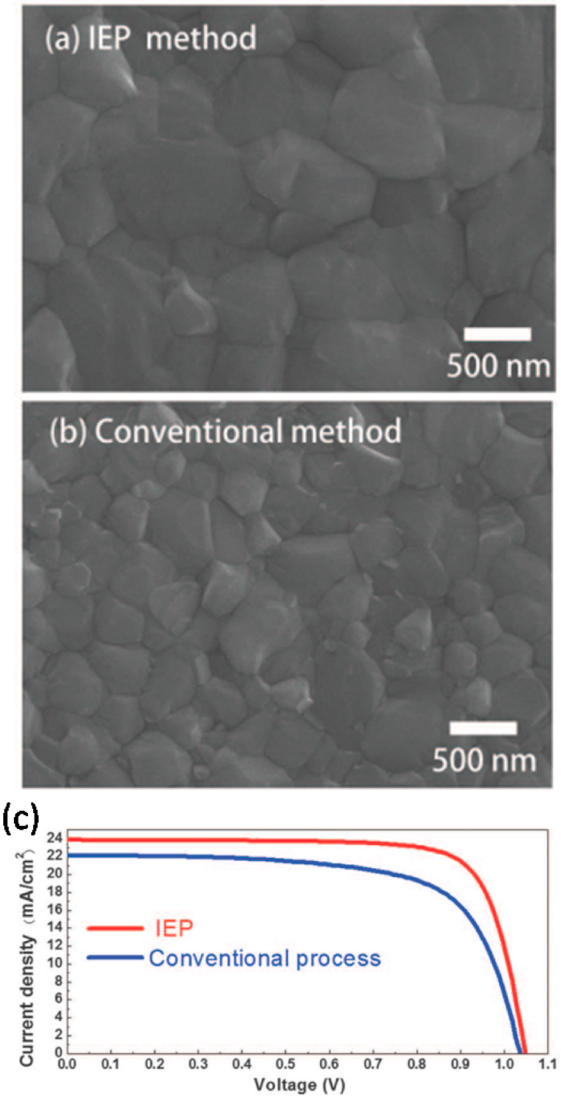

Figure 4. (a,b) Scanning electron microscopy images of lead halide perovskite films prepared using an intramolecular exchange process (IEP) and a two-step interdiffusion method (conventional). (c) Current density–voltage curves of solar cell devices made from films shown in (a) and (b). Reproduced with permission from ref 2. Copyright American Association for the Advancement of Science.

DOI: 10.1021/jacs.5b10723
J. Am. Chem. Soc. 2016, 138, 463–470

thermodynamics or kinetics of film formation in such a way as to promote the formation of larger grains, but this processes is likely assisted by the existing PbI_2–DMSO lattice, which could drastically lower the energy barrier for perovskite formation.

5. COMPOSITIONAL ENGINEERING

While the vast majority of lead halide perovskite work has focused on the $MAPbI_3$ system, perovskites with other organic cations or halide ions have also been investigated. Eperon et al. were the first to fabricate a high-efficiency perovskite solar cell using the formamidinium (FA) cation.[29] The FA cation is larger than the MA cation and leads to a reduced band gap compared to the $MAPbI_3$ system, 1.57 to 1.48 eV, making it better suited for application in a single junction solar cell. Eperon and co-workers also demonstrated that, by using FA and substituting bromine for iodide, lead halide perovskite films with tunable band gaps from 1.48 to 2.23 eV could be fabricated. Perovskite solar cells incorporating FA have been shown to be more thermally stable than MA devices,[29] whereas the substitution of some amount of iodide with bromide has been shown to limit device degradation in humid environments,[49] but perhaps at the expense of light stability.[50] Mixed-cation perovskite systems incorporating both FA and MA have also been incorporated into relatively efficient solar cell devices.[51,52] Jeon et al. extended this compositional engineering strategy by fabricating lead halide perovskite solar cells consisting of a mixture of $FAPbI_3$ and the tribromide perovskite $MAPbBr_3$.[53] $MAPbBr_3$ was shown to increase the stability of the perovskite phase of $FAPbI_3$ and lead to higher PCEs. Many questions remain about this mixed-phase engineering, such as how homogeneous the phase distribution is throughout the film, and how this distribution affects film optoelectronic properties?[50] Due to concerns over lead toxicity, attempts have been made to replace lead with tin, but the resulting solar cells exhibit much decreased PCE.[54,55] Due to $MAPbI_3$-based devices' thermal instability, the identification of new cation/halide combinations is likely important for future commercialization efforts of lead halide perovskite solar cells. Such thermal stability could be achieved by using fully inorganic perovskite materials. By replacing the organic cation with the inorganic cesium ion, greater thermal stability is achieved, but this substitution drastically lowers device efficiency, and the resulting highly absorbing cubic $CsPbI_3$ phase exhibits significant instability in air.[56]

6. HUMIDITY

As perovskite precursor materials and also lead halide perovskites exhibit some degree of solubility in water, it has been suspected that the presence of water vapor during film fabrication may influence film formation.[57] This effect, however, has not been carefully investigated until recently. Work by Eperon et al. on $MAPbI_3$ films and solar cells has shown that lead halide perovskite films fabricated in a humid environment have a lower trap-state density and therefore higher photoluminescence (PL) and longer PL lifetimes compared to films fabricated in a dry environment.[58] The effect of water is more nuanced than these improvements imply, however, as water vapor also seems to lead to a more discontinuous film with poorer surface coverage.[58,59] The work to date then suggests that it may be undesirable to spin-coat $MAPbI_3$ films in a humid environment, as this will lead to poor surface coverage when using the one-step fabrication protocol, but that annealing spin-cast films in a humid environment is a useful strategy to improve films' optoelectronic properties and produce high-efficiency devices.[60] Yang and co-workers demonstrated that perovskite films produced using the interdiffusion bilayer protocol developed much larger grains when exposed to humid air before thermal annealing compared to devices fabricated in a dry nitrogen glove box.[61] This is very similar to the solvent annealing effect Xiao et al. demonstrated using DMF and DMSO (discussed more below).[62] It is therefore possible that fabrication in a humid environment is a type of solvent annealing treatment. As suggested by Eperon et al., the improvement in device optoelectronic properties with exposure to humidity may be due to favorable interactions between water and MAI.[58] This may be why it has been observed that carrier lifetime, open-circuit voltage, and fill factor decrease with increasing humidity levels during film preparation for $FAPbI_3$ films and devices.[63] While exposure to elevated levels of humidity has been shown to be advantageous to the growth of $MAPbI_3$ films with desirable optoelectronic properties, extended water vapor exposure to fully formed perovskite films will accelerate their degradation.[64−66] Great care should therefore be taken to control the humidity levels during film processing, characterization, and long-term operation, as humidity is deleterious to MA-based devices during spin-coating and long-term operation but beneficial during film annealing. Humidity appears to be deleterious to FA-based devices at all times. This difference should be kept in mind during the development and evaluation of future cations.

7. GRAIN BOUNDARIES, SURFACES, AND HETEROGENEITY

In part because they are formed from low-temperature thermal evaporation or, more commonly, solution-based processes, lead halide perovskite thin films are polycrystalline. Therefore, they contain grain boundaries, the density of which depends on the size and shape of the perovskite grains. First-principle calculations have suggested that lead halide perovskite grain boundaries are intrinsically benign, leading to single crystal-like behavior for polycrystalline films.[67] Experimental work, however, has shown that grain boundaries significantly affect thin-film optoelectronic properties. Xiao et al. thermally annealed interdiffusion bilayer fabricated perovskite films in the presence of DMF vapor to fabricate $MAPbI_3$ films with grains roughly the size of the thickness of the films (Figure 5).[62] The short-circuit current density and fill factor of solar cells made from these films remained very high even when films were made over 1 μm thick, whereas films that were not

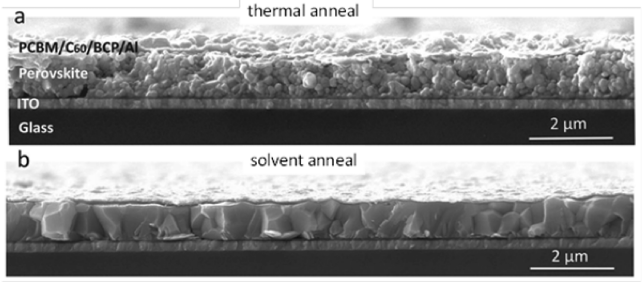

Figure 5. Cross-sectional scanning electron microscopy of $MAPbI_3$ films fabricated using thermal annealing (a) and solvent annealing (b) protocols. Reprinted with permission from ref 62. Copyright 2014 John Wiley and Sons.

DOI: 10.1021/jacs.5b10723
J. Am. Chem. Soc. 2016, 138, 463−470

annealed in the presence of solvent vapor exhibited a decrease in both figures of merit when the film thickness exceeded the grain size. This observation strongly suggests that solar cell performance is increased when charge carriers are able to diffuse the thickness of the film without encountering a grain boundary. Likewise, Tosun and Hillhouse were able to dramatically increase grain size by annealing perovskite films in a Teflon pressure vessel containing MAI vapor.[68] These larger grained films exhibited much longer PL lifetimes. These examples suggest thin-film perovskite optoelectronic properties can be optimized by minimizing grain boundaries via the formation of large-grained films.

The effect of lead halide perovskite surfaces on optoelectronic properties has also been investigated with theory and experimental work. Theoretical studies have suggested that perovskite surfaces maintain bulk-like characteristics, implying they should not negatively impact optoelectronic properties.[69,70] Experimental work suggests this claim may have some validity. Yang et al. investigated the surface recombination velocity of $MAPbBr_3$ single crystals and found it to be 2−3 orders of magnitude lower than that of many other semiconductors currently used in commercial solar cells.[71] Those authors suggest, however, that perovskite films with grains smaller than 5 μm, encompassing most lead halide perovskite films fabricated to date, will likely require surface passivation to avoid reductions in carrier lifetime. Accordingly, device performance can be increased by incorporating a fullerene interlayer as fullerenes are capable of partially passivating surface traps and in doing so lead to lower trap densities.[25,72,73] Additionally, the Snaith group has demonstrated that both solar cell performance and PL lifetimes improve when perovskite surfaces were passivated either with a Lewis base such as thiophene or pyridine[74] or with supramolecular halogen bond complexation.[75] Those authors hypothesized that these strategies are able to compensate for under-coordinated lead and halide surface sites, respectively, thus passivating electronic surface traps. This work was extended by using confocal fluorescence microscopy to spatially resolve PL decay dynamics on $PbCl_2$-derived perovskite films treated with and without pyridine vapor (Figure 6).[76] It was found that some grains exhibited brighter PL than others and that grain boundaries were darker than grain interiors, again suggesting grain boundaries' deleterious optoelectronic effect. Brighter grains seemed to correlate with residual chlorine present in the film, and pyridine treatment was shown to activate previously dark grains. These results suggest that, at least in the $PbCl_2$-derived case, perovskite films are morphologically and optoelectronically heterogeneous, that grain boundaries are detrimental to optoelectronic properties, and that a tailored surface treatment is capable of to some degree passivating these problems. Vrućinić et al. then revealed heterogeneous PL brightness in perovskite films fabricated without any chloride containing precursors, suggesting chloride ions are not uniquely responsible for this phenomenon.[77] Similarly, Bischak and coworkers used cathodoluminescence microscopy to reveal significant differences in nonradiative recombination rates from grain to grain within a solvent-engineered perovskite thin film.[78] Stone and Tassone have also shown solution-processed lead halide perovskites to be heterogeneous. Using a combination of X-ray diffraction techniques, they were able to determine that perovskite films made via a solvent engineering technique were approximately 30% amorphous by volume.[79] This is surprising given the lack of obviously disordered regions

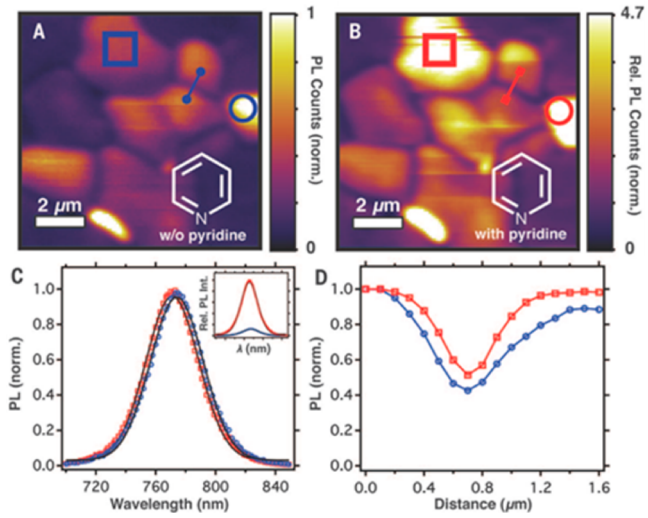

Figure 6. (A,B) Fluorescence microscopy images of $PbCl_2$-derived $MAPbI_3$ films with and without pyridine vapor treatment. (C) Inset: Bulk steady-state PL spectra showing relative PL intensities before (blue circle) and after (red square) treatment. Main figure: normalized PL spectra of same. (D) Grain boundary PL line scan before and after treatment (blue and red lines in (A) and (B), respectively). Reprinted with permission from ref 76. Copyright 2015 American Association for the Advancement of Science.

in film scanning electron microscopy images. The spatial distribution of this amorphous vs crystalline content within the film is unknown. It is also unknown whether fabrication protocols that seem to produce very crystalline, large-grained films when examined by scanning electron microscopy such as solvent annealing contain these amorphous regions. Presumably, eliminating this amorphous fraction could lead to improved device PCE.

8. CONCLUSIONS

Perhaps one of the most surprising findings of the perovskite revolution is the diversity of fabrication approaches that can be used to produce lead halide perovskite thin films. While many different techniques can be used to produce lead halide perovskite thin films, only a few are capable of producing the morphology necessary for efficient thin-film solar cells. In general, lead halide perovskite films need to be smooth, continuous, and have micrometer-sized grains in order to produce high-efficiency solar cells.[2,20] Such films can be produced when care is taken to first promote uniform nucleation of the lead precursor (two-step) or perovskite (one-step) across the substrate and then encourage growth. As discussed at length above this can be accomplished multiple ways, such as first depositing a PbI_2 film and then converting it to perovskite, by using solvent additives to modify the lead precursor solubility, by accelerating the drying rate during film casting, or by forming solvent−precursor complexes that are then converted to the lead halide perovskite. Rough, discontinuous, and/or severely heterogeneous films are produced when the PbI_2 film morphology is not carefully controlled when using a two-step method, by not carefully controlling the solubility of precursors in solution when using a one-step method, and/or by not carefully controlling the humidity of the processing environment. Clearly, lead halide perovskite morphology is extremely sensitive to the environ-

DOI: 10.1021/jacs.5b10723
J. Am. Chem. Soc. 2016, 138, 463−470

mental and experimental conditions at each step of the fabrication process.

More needs to be done in order to understand the general conditions that produce large-grained perovskite films. Given the strong correlation between improved optoelectronic properties and increased gain size,[2,19,20,62,68] micrometer-sized grains seem to be an important morphological feature for high-efficiency perovskite solar cells. This need may be exacerbated by the large-area devices used in commercial modules, where lateral charge carrier diffusion over longer length scales often becomes necessary for charge collection at electrodes. Work on scalable, large-area fabrication techniques is also essential for the successful commercialization of this technology.[47,80,81] Importantly, this work should be guided by the processing−property−performance relationships elucidated here on spin-coated, small-area films. Additionally, more work needs to be done in order to understand and characterize the structural heterogeneity of perovskite films suggested by recent work. Eliminating this heterogeneity may very well be crucial to maximizing the potential of this class of materials. Much has been learned about this relatively new class of materials in an amazingly short period of time, but further processing−property−performance relationships must be developed before lead halide perovskite solar cells approaching their thermodynamic efficiency limit can be easily and reproducibly fabricated.

AUTHOR INFORMATION

Corresponding Authors

*sharenko@slac.stanfored.edu

*mftoney@slac.stanford.edu

Notes

The authors declare no competing financial interest.

ACKNOWLEDGMENTS

This work was supported by the Laboratory Directed Research and Development Program at SLAC under contract DE-AC02-76-SF00515 (Lead Halide Perovskite Photovoltaic Thin Films: Processing, Crystallization Dynamics and Morphology). Use of the Stanford Synchrotron Radiation Lightsource, SLAC National Accelerator Laboratory, is supported by the U.S. Department of Energy, Office of Science, Office of Basic Energy Sciences, under contract DE-AC02-76SF00515. We thank Aryeh Gold-Parker for helpful discussions and Vanessa Pool for the table of contents image.

REFERENCES

(1) Berry, J.; Buonassisi, T.; Egger, D. A.; Hodes, G.; Kronik, L.; Loo, Y.-L.; Lubomirsky, I.; Marder, S. R.; Mastai, Y.; Miller, J. S.; Mitzi, D. B.; Paz, Y.; Rappe, A. M.; Riess, I.; Rybtchinski, B.; Stafsudd, O.; Stevanovic, V.; Toney, M. F.; Zitoun, D.; Kahn, A.; Ginley, D.; Cahen, D. *Adv. Mater.* **2015**, *27*, 5102−5112.

(2) Yang, W. S.; Noh, J. H.; Jeon, N. J.; Kim, Y. C.; Ryu, S.; Seo, J.; Seok, S. I. *Science* **2015**, *348*, 1234.

(3) Green, M. A.; Emery, K.; Hishikawa, Y.; Warta, W.; Dunlop, E. D. *Prog. Photovoltaics* **2015**, *23* (7), 805−812.

(4) De Wolf, S.; Holovsky, J.; Moon, S.-J.; Löper, P.; Niesen, B.; Ledinsky, M.; Haug, F.-J.; Yum, J.-H.; Ballif, C. *J. Phys. Chem. Lett.* **2014**, *5* (6), 1035−1039.

(5) Yin, W.-J.; Shi, T.; Yan, Y. *Appl. Phys. Lett.* **2014**, *104* (6), 063903.

(6) Kim, J.; Lee, S.-H.; Lee, J. H.; Hong, K.-H. *J. Phys. Chem. Lett.* **2014**, *5*, 1312−1317.

(7) Tress, W.; Marinova, N.; Moehl, T.; Zakeeruddin, S. M.; Nazeeruddin, M. K.; Grätzel, M. *Energy Environ. Sci.* **2015**, *8* (3), 995−1004.

(8) Snaith, H. J.; Abate, A.; Ball, J. M.; Eperon, G. E.; Leijtens, T.; Noel, N. K.; Stranks, S. D.; Wang, J. T.-W.; Wojciechowski, K.; Zhang, W. *J. Phys. Chem. Lett.* **2014**, *5* (9), 1511−1515.

(9) Niu, G.; Guo, X.; Wang, L. *J. Mater. Chem. A* **2015**, *3* (17), 8970−8980.

(10) Leijtens, T.; Eperon, G. E.; Noel, N. K.; Habisreutinger, S. N.; Petrozza, A.; Snaith, H. J. *Adv. Energy Mater.* **2015**, *5*, 00963.

(11) Snaith, H. J. *J. Phys. Chem. Lett.* **2013**, *4* (21), 3623−3630.

(12) Liang, K.; Mitzi, D. B.; Prikas, M. T. *Chem. Mater.* **1998**, *10* (1), 403−411.

(13) Burschka, J.; Pellet, N.; Moon, S.-J.; Humphry-Baker, R.; Gao, P.; Nazeeruddin, M. K.; Grätzel, M. *Nature* **2013**, *499* (7458), 316−319.

(14) Liu, D.; Kelly, T. L. *Nat. Photonics* **2014**, *8* (2), 133−138.

(15) Wu, Y.; Islam, A.; Yang, X.; Qin, C.; Liu, J.; Zhang, K.; Peng, W.; Han, L. *Energy Environ. Sci.* **2014**, *7* (9), 2934−2938.

(16) Yang, L.; Wang, J.; Leung, W. W.-F. *ACS Appl. Mater. Interfaces* **2015**, *7* (27), 14614−14619.

(17) Xiao, Z.; Bi, C.; Shao, Y.; Dong, Q.; Wang, Q.; Yuan, Y.; Wang, C.; Gao, Y.; Huang, J. *Energy Environ. Sci.* **2014**, *7*, 2619−2623.

(18) Bi, C.; Shao, Y.; Yuan, Y.; Xiao, Z.; Wang, C.; Gao, Y.; Huang, J. *J. Mater. Chem. A* **2014**, *2* (43), 18508−18514.

(19) Bi, C.; Wang, Q.; Shao, Y.; Yuan, Y.; Xiao, Z.; Huang, J. *Nat. Commun.* **2015**, *6*, 7747.

(20) Dong, Q.; Yuan, Y.; Shao, Y.; Fang, Y.; Wang, Q.; Huang, J. *Energy Environ. Sci.* **2015**, *8* (8), 2464−2470.

(21) Tidhar, Y.; Edri, E.; Weissman, H.; Zohar, D.; Hodes, G.; Cahen, D.; Rybtchinski, B.; Kirmayer, S. *J. Am. Chem. Soc.* **2014**, *136* (38), 13249−13256.

(22) Wu, C.-G.; Chiang, C.-H.; Tseng, Z.-L.; Nazeeruddin, M. K.; Hagfeldt, A.; Grätzel, M. *Energy Environ. Sci.* **2015**, *8*, 2725−2733.

(23) Liu, M.; Johnston, M. B.; Snaith, H. J. *Nature* **2013**, *501* (7467), 395−398.

(24) Eperon, G. E.; Burlakov, V. M.; Docampo, P.; Goriely, A.; Snaith, H. J. *Adv. Funct. Mater.* **2014**, *24* (1), 151−157.

(25) Wang, Q.; Shao, Y.; Dong, Q.; Xiao, Z.; Yuan, Y.; Huang, J. *Energy Environ. Sci.* **2014**, *7* (7), 2359−2365.

(26) Yan, K.; Long, M.; Zhang, T.; Wei, Z.; Chen, H.; Yang, S.; Xu, J. *J. Am. Chem. Soc.* **2015**, *137*, 4460−4468.

(27) Liang, P.-W.; Liao, C.-Y.; Chueh, C.-C.; Zuo, F.; Williams, S. T.; Xin, X.-K.; Lin, J.; Jen, A. K.-Y. *Adv. Mater.* **2014**, *26*, 3748−3754.

(28) Chueh, C.-C.; Liao, C.-Y.; Zuo, F.; Williams, S. T.; Liang, P.-W.; Jen, A. K.-Y. *J. Mater. Chem. A* **2015**, *3*, 9058−9062.

(29) Eperon, G. E.; Stranks, S. D.; Menelaou, C.; Johnston, M. B.; Herz, L. M.; Snaith, H. J. *Energy Environ. Sci.* **2014**, *7* (3), 982−988.

(30) Heo, J.-H.; Han, H. J.; Kim, D.; Ahn, T.; Im, S. H. *Energy Environ. Sci.* **2015**, *8*, 1602−1608.

(31) Heo, J. H.; Song, D. H.; Han, H. J.; Kim, S. Y.; Kim, J. H.; Kim, D.; Shin, H. W.; Ahn, T. K.; Wolf, C.; Lee, T.-W.; Im, S. H. *Adv. Mater.* **2015**, *27*, 3424−3430.

(32) Li, G.; Zhang, T.; Zhao, Y. *J. Mater. Chem. A* **2015**, *3* (39), 19674−19678.

(33) Stamplecoskie, K. G.; Manser, J. S.; Kamat, P. V. *Energy Environ. Sci.* **2015**, *8* (1), 208−215.

(34) Williams, S. T.; Zuo, F.; Chueh, C.-C.; Liao, C.-Y.; Liang, P.-W.; Jen, A. K.-Y. *ACS Nano* **2014**, *8* (10), 10640−10654.

(35) Stranks, S. D.; Eperon, G. E.; Grancini, G.; Menelaou, C.; Alcocer, M. J. P.; Leijtens, T.; Herz, L. M.; Petrozza, A.; Snaith, H. J. *Science* **2013**, *342* (6156), 341−344.

(36) Colella, S.; Mosconi, E.; Fedeli, P.; Listorti, A.; Gazza, F.; Orlandi, F.; Ferro, P.; Besagni, T.; Rizzo, A.; Calestani, G.; Gigli, G.; De Angelis, F.; Mosca, R. *Chem. Mater.* **2013**, *25* (22), 4613−4618.

(37) Yu, H.; Wang, F.; Xie, F.; Li, W.; Chen, J.; Zhao, N. *Adv. Funct. Mater.* **2014**, *24* (45), 7102−7108.

(38) Unger, E. L.; Bowring, A. R.; Tassone, C. J.; Pool, V. L.; Gold-Parker, A.; Cheacharoen, R.; Stone, K. H.; Hoke, E. T.; Toney, M. F.; McGehee, M. D. *Chem. Mater.* **2014**, *26* (24), 7158−7165.

(39) Zhang, W.; Saliba, M.; Moore, D. T.; Pathak, S. K.; Hörantner, M. T.; Stergiopoulos, T.; Stranks, S. D.; Eperon, G. E.; Alexander-

DOI: 10.1021/jacs.5b10723
J. Am. Chem. Soc. 2016, 138, 463−470

Webber, J. A.; Abate, A.; Sadhanala, A.; Yao, S.; Chen, Y.; Friend, R. H.; Estroff, L. A.; Wiesner, U.; Snaith, H. J. *Nat. Commun.* **2015**, *6*, 6142.
(40) Starr, D. E.; Sadoughi, G.; Handick, E.; Wilks, R. G.; Alsmeier, J. H.; Köhler, L.; Gorgoi, M.; Snaith, H. J.; Bär, M. *Energy Environ. Sci.* **2015**, *8* (5), 1609−1615.
(41) Li, Y.; Sun, W.; Yan, W.; Ye, S.; Peng, H.; Liu, Z.; Bian, Z.; Huang, C. *Adv. Funct. Mater.* **2015**, *25* (30), 4867−4873.
(42) Pool, V. L.; Gold-Parker, A.; McGehee, M. D.; Toney, M. F. *Chem. Mater.* **2015**, *27*, 7240.
(43) Moore, D. T.; Sai, H.; Tan, K. W.; Smilgies, D.-M.; Zhang, W.; Snaith, H. J.; Wiesner, U.; Estroff, L. A. *J. Am. Chem. Soc.* **2015**, *137*, 2350−2358.
(44) Jeon, N. J.; Noh, J. H.; Kim, Y. C.; Yang, W. S.; Ryu, S.; Seok, S. I. *Nat. Mater.* **2014**, *13* (9), 897−903.
(45) Ahn, N.; Son, D.-Y.; Jang, I.-H.; Kang, S. M.; Choi, M.; Park, N.-G. *J. Am. Chem. Soc.* **2015**, *137* (27), 8696−8699.
(46) Huang, F.; Dkhissi, Y.; Huang, W.; Xiao, M.; Benesperi, I.; Rubanov, S.; Zhu, Y.; Lin, X.; Jiang, L.; Zhou, Y.; Gray-Weale, A.; Etheridge, J.; McNeill, C. R.; Caruso, R. A.; Bach, U.; Spiccia, L.; Cheng, Y.-B. *Nano Energy* **2014**, *10*, 10−18.
(47) Deng, Y.; Peng, E.; Shao, Y.; Xiao, Z.; Dong, Q.; Huang, J. *Energy Environ. Sci.* **2015**, *8* (5), 1544−1550.
(48) Xiao, M.; Huang, F.; Huang, W.; Dkhissi, Y.; Zhu, Y.; Etheridge, J.; Gray-Weale, A.; Bach, U.; Cheng, Y.-B.; Spiccia, L. *Angew. Chem.* **2014**, *126* (37), 10056−10061.
(49) Noh, J. H.; Im, S. H.; Heo, J. H.; Mandal, T. N.; Seok, S. I. *Nano Lett.* **2013**, *13* (4), 1764−1769.
(50) Hoke, E. T.; Slotcavage, D. J.; Dohner, E. R.; Bowring, A. R.; Karunadasa, H. I.; McGehee, M. D. *Chem. Sci.* **2015**, *6* (1), 613−617.
(51) Pellet, N.; Gao, P.; Gregori, G.; Yang, T.-Y.; Nazeeruddin, M. K.; Maier, J.; Grätzel, M. *Angew. Chem., Int. Ed.* **2014**, *53* (12), 3151−3157.
(52) Liu, J.; Shirai, Y.; Yang, X.; Yue, Y.; Chen, W.; Wu, Y.; Islam, A.; Han, L. *Adv. Mater.* **2015**, *27*, 4918−4923.
(53) Jeon, N. J.; Noh, J. H.; Yang, W. S.; Kim, Y. C.; Ryu, S.; Seo, J.; Seok, S. I. *Nature* **2015**, *517* (7535), 476−480.
(54) Hao, F.; Stoumpos, C. C.; Cao, D. H.; Chang, R. P. H.; Kanatzidis, M. G. *Nat. Photonics* **2014**, *8* (6), 489−494.
(55) Noel, N. K.; Stranks, S. D.; Abate, A.; Wehrenfennig, C.; Guarnera, S.; Haghighirad, A.; Sadhanala, A.; Eperon, G. E.; Pathak, S. K.; Johnston, M. B.; Petrozza, A.; Herz, L.; Snaith, H. *Energy Environ. Sci.* **2014**, *7*, 3061−3068.
(56) Eperon, G. E.; Paternò, G. M.; Sutton, R. J.; Zampetti, A.; Haghighirad, A. A.; Cacialli, F.; Snaith, H. J. *J. Mater. Chem. A* **2015**, *3* (39), 19688−19695.
(57) Egger, D. A.; Edri, E.; Cahen, D.; Hodes, G. *J. Phys. Chem. Lett.* **2015**, *6* (2), 279−282.
(58) Eperon, G. E.; Habisreutinger, S. N.; Leijtens, T.; Bruijnaers, B. J.; van Franeker, J. J.; deQuilettes, D. W.; Pathak, S.; Sutton, R. J.; Grancini, G.; Ginger, D. S.; Janssen, R. A. J.; Petrozza, A.; Snaith, H. J. *ACS Nano* **2015**, *9*, 9380−9393.
(59) Gao, H.; Bao, C.; Li, F.; Yu, T.; Yang, J.; Zhu, W.; Zhou, X.; Fu, G.; Zou, Z. *ACS Appl. Mater. Interfaces* **2015**, *7* (17), 9110−9117.
(60) You, J.; Yang, Y.; Hong, Z.; Song, T.-B.; Meng, L.; Liu, Y.; Jiang, C.; Zhou, H.; Chang, W.-H.; Li, G.; Yang, Y. *Appl. Phys. Lett.* **2014**, *105* (18), 183902.
(61) Yang, B.; Dyck, O.; Poplawsky, J.; Keum, J.; Puretzky, A.; Das, S.; Ivanov, I.; Rouleau, C.; Duscher, G.; Geohegan, D.; Xiao, K. *J. Am. Chem. Soc.* **2015**, *137* (29), 9210−9213.
(62) Xiao, Z.; Dong, Q.; Bi, C.; Shao, Y.; Yuan, Y.; Huang, J. *Adv. Mater.* **2014**, *26* (37), 6503−6509.
(63) Wozny, S.; Yang, M.; Nardes, A. M.; Mercado, C. C.; Ferrere, S.; Reese, M. O.; Zhou, W.; Zhu, K. *Chem. Mater.* **2015**, *27* (13), 4814−4820.
(64) Leguy, A. M. A.; Hu, Y.; Campoy-Quiles, M.; Alonso, M. I.; Weber, O. J.; Azarhoosh, P.; van Schilfgaarde, M.; Weller, M. T.; Bein, T.; Nelson, J.; Docampo, P.; Barnes, P. R. F. *Chem. Mater.* **2015**, *27* (9), 3397−3407.
(65) Yang, J.; Siempelkamp, B. D.; Liu, D.; Kelly, T. L. *ACS Nano* **2015**, *9*, 1955−1963.
(66) Christians, J. A.; Miranda Herrera, P. A.; Kamat, P. V. *J. Am. Chem. Soc.* **2015**, *137* (4), 1530−1538.
(67) Yin, W.-J.; Shi, T.; Yan, Y. *Adv. Mater.* **2014**, *26* (27), 4653−4658.
(68) Tosun, B. S.; Hillhouse, H. W. *J. Phys. Chem. Lett.* **2015**, *6* (13), 2503−2508.
(69) Haruyama, J.; Sodeyama, K.; Han, L.; Tateyama, Y. *J. Phys. Chem. Lett.* **2014**, *5* (16), 2903−2909.
(70) Buin, A.; Pietsch, P.; Xu, J.; Voznyy, O.; Ip, A. H.; Comin, R.; Sargent, E. H. *Nano Lett.* **2014**, *14* (11), 6281−6286.
(71) Yang, Y.; Yan, Y.; Yang, M.; Choi, S.; Zhu, K.; Luther, J. M.; Beard, M. C. *Nat. Commun.* **2015**, *6*, 7961.
(72) Shao, Y.; Xiao, Z.; Bi, C.; Yuan, Y.; Huang, J. *Nat. Commun.* **2014**, *5*, 5784.
(73) Xu, J.; Buin, A.; Ip, A. H.; Li, W.; Voznyy, O.; Comin, R.; Yuan, M.; Jeon, S.; Ning, Z.; McDowell, J. J.; Kanjanaboos, P.; Sun, J.-P.; Lan, X.; Quan, L. N.; Kim, D. H.; Hill, I. G.; Maksymovych, P.; Sargent, E. H. *Nat. Commun.* **2015**, *6*, 7081.
(74) Noel, N. K.; Abate, A.; Stranks, S. D.; Parrott, E. S.; Burlakov, V. M.; Goriely, A.; Snaith, H. J. *ACS Nano* **2014**, *8*, 9815−9821.
(75) Abate, A.; Saliba, M.; Hollman, D. J.; Stranks, S. D.; Wojciechowski, K.; Avolio, R.; Grancini, G.; Petrozza, A.; Snaith, H. J. *Nano Lett.* **2014**, *14* (6), 3247−3254.
(76) de Quilettes, D. W.; Vorpahl, S. M.; Stranks, S. D.; Nagaoka, H.; Eperon, G. E.; Ziffer, M. E.; Snaith, H. J.; Ginger, D. S. *Science* **2015**, *348* (6235), 683−686.
(77) Vrućinić, M.; Matthiesen, C.; Sadhanala, A.; Divitini, G.; Cacovich, S.; Dutton, S. E.; Ducati, C.; Atatüre, M.; Snaith, H.; Friend, R. H.; Sirringhaus, H.; Deschler, F. *Adv. Sci.* **2015**, *2* (9), 00136.
(78) Bischak, C. G.; Sanehira, E. M.; Precht, J. T.; Luther, J. M.; Ginsberg, N. S. *Nano Lett.* **2015**, *15* (7), 4799−4807.
(79) Stone, K. H., Tassone, C. J., private communication.
(80) Yang, Z.; Chueh, C.-C.; Zuo, F.; Kim, J. H.; Liang, P.-W.; Jen, A. K.-Y. *Adv. Energy Mater.* **2015**, *5*, 1500328.
(81) Das, S.; Yang, B.; Gu, G.; Joshi, P. C.; Ivanov, I. N.; Rouleau, C. M.; Aytug, T.; Geohegan, D. B.; Xiao, K. *ACS Photonics* **2015**, *2* (6), 680−686.

DOI: 10.1021/jacs.5b10723
J. Am. Chem. Soc. 2016, 138, 463−470